

## Angular and chromatic dispersion in Kerr-driven conical emission

Daniele Faccio<sup>a,\*</sup>, Miguel Angel Porras<sup>b</sup>, Audrius Dubietis<sup>c</sup>, Gintaras Tamošauskas<sup>c</sup>, Ernestas Kučinskas<sup>c</sup>, Arnaud Couairon<sup>d</sup>, Paolo Di Trapani<sup>a</sup>

<sup>a</sup> INFN and Department of Physics and Mathematics, University of Insubria, Via Valleggio 11, 22100 Como, Italy

<sup>b</sup> Departamento de Física Aplicada, ETSIM, Universidad Politécnica de Madrid, Ríos Rosas 21, 28003 Madrid, Spain

<sup>c</sup> Department of Quantum Electronics, Vilnius University, Sauletekio Ave. 9, Bldg. 3, LT-10222, Vilnius, Lithuania

<sup>d</sup> Centre de Physique Théorique, Ecole Polytechnique, CNRS UMR 7644, F-91128 Palaiseau, France

Received 16 March 2006; received in revised form 6 April 2006; accepted 6 April 2006

### Abstract

We report measurements of ultrashort optical pulse filamentation in Kerr media with normal dispersion. We measure the angular dispersion of spontaneously generated colored conical emission and show that for large frequency shifts from the input pump frequency, it is well described by a relation between angle and frequency with slope determined solely by material chromatic dispersion. This measurement is in agreement with recent models that interpret filamentation dynamics in terms of the spontaneous formation of nonlinear X-waves. Finally, experimental results of filamentation in air show, for the first time, that the interpretation of CE in terms of X-waves may be also extended to gaseous media.

© 2006 Elsevier B.V. All rights reserved.

Wave collapse of ultrashort laser pulses and the more generically referred to phenomenon of filamentation are proving to be ground of fertile physical debates due both to potential applications [1–3] and to the similarity of the governing equation, the nonlinear Schrödinger equation (NSE), with that of other experimentally less accessible systems, such as Bose–Einstein condensates [4]. In the case of self-focusing and optical wave collapse in third-order (Kerr) nonlinear media, the very high intensities reached during the process typically require to modify the NSE with the inclusion of extra terms (accounting for nonlinear absorption, higher order saturating nonlinearities, plasma generation, Raman scattering, etc. [5]), in order to properly account for the detailed complexity observed in the experiments. In spite of that, the “geometrical” features of wave-packet dynamics, leading to conical emission (CE) [6–8], to nonlinear X-wave generation [9] and, more generally, to all the nontrivial manifestations of spatio-temporal coupling, are forecasted to be essentially dictated by the linear terms

in the equation, i.e., by the interplay of diffraction and chromatic dispersion [10,11]. We stress that the need for properly accounting of both spatial and temporal degrees of freedom has been pointed out since more than a decade for what concerns theoretical and numerical investigations [11]. Only recently, new experimental techniques have been proposed suitable for reconstructing the near-field spatio-temporal intensity profile [12], the far-field angular spectrum [13] and the three-dimensional amplitude and phase field distribution [14].

CE and in general continuum generation are peculiar to optical wave collapse and are observed as a strong on-axis spectral broadening and newly generated spectral components emitted on radially symmetric cones centered on the beam propagation axis [10,15]. In particular it has been predicted that the angular dispersion (AD) of the CE in normally dispersive media follows a relation given by [10]

$$\theta = \sqrt{k_0''/k_0} \Omega \quad (1)$$

where  $\theta$  is the propagation angle with respect to the input pump beam axis,  $k_0 = 2\pi n/\lambda_0$  ( $\lambda_0$  is the input pump wavelength and  $n$  the refractive index),  $k_0'' = \partial^2 k/\partial \omega^2|_{\omega_0}$  and

\* Corresponding author. Tel.: +39 312386221; fax: +39 312386209.  
E-mail address: [daniele.faccio@uninsubria.it](mailto:daniele.faccio@uninsubria.it) (D. Faccio).

$\Omega = \omega - \omega_0$  is the difference between the generated frequency and the input pump frequency. This relation was deduced supposing that CE is generated by a four-wave mixing (FWM) process in the NSE dynamics. However, to date, experimental quantitative verification of this relation is still lacking.

More recently a somewhat different interpretation of filamentation dynamics has emerged. It has been demonstrated that Gaussian wave packets during filamentation process spontaneously reshape into conical waves [16], and those are unbalanced Bessel beams in the continuous wave limit [17] and nonlinear X-waves in the ultrashort pulse regime [9]. The nonlinear X-waves are conical waves with the important characteristic of stationary non-dispersive and non-diffractive propagation [18]. The successive filamentation dynamics, CE and in particular the X-shaped spectrum observed in the  $(k_{\perp}, \Omega)$  (or  $(\theta, \lambda)$ ) space are explained as an explicit manifestation of these nonlinear X-waves [19,20]. Moreover it has been noted that much information may be obtained regarding even the near-field distributions from a careful analysis of the far-field  $(\theta, \lambda)$  spectrum [13,21]. In the far-field it is possible to write out the form of the X spectrum explicitly in a simple analytical form [22]:

$$\theta = \sqrt{\frac{2}{k_0} \left( \beta + \alpha\Omega + \frac{1}{2} k_0'' \Omega^2 \right)} \quad (2)$$

where  $\beta$  and  $\alpha$  are two parameters related to the phase and group velocities, respectively, of the X-wave [22]. An interesting feature of this equation is that for large  $\Omega$  it reduces to Eq. (1), thus highlighting a clear link between the two interpretations, i.e., that of a phase-matched FWM process and the spontaneous formation of nonlinear X-waves. We also note here that linear and nonlinear X-waves have common features. Among them, there is the asymptotic (i.e., for large  $\Omega$ ) part of the far-field spectrum, justifying the use of Eq. (2) and similar forms for wave-packets that are interpreted as a manifestation of spontaneously generated nonlinear X-waves.

In this work we induce filamentation of 200 fs laser pulses in water and by using a precise spectrographic imaging technique we characterize the CE in the angle–wavelength  $(\theta, \lambda)$  space. We demonstrate that a linear relation with slope  $\sqrt{k_0''/k_0}$  describes our data quite accurately for large  $\Omega$ . We also find an asymmetry between red- and blue-shifted CE that is accounted for with a third-order dispersion correction, further supporting that CE structure is determined by linear dispersion. In addition, observed intensity-dependent structure of CE at high input energies finds also explanation within this frame once plasma correction to  $k_0''$  is taken into account. Measurements are also performed in air, therefore extending to gaseous media the interpretation of filamentation dynamics on the basis of a spontaneous generation of nonlinear X-waves.

The experiments were carried out in various Kerr media: water, air and a lithium-triborate (LBO) crystal. The input

laser pulse was delivered from a 10 Hz Nd:glass mode-locked and regeneratively amplified system (Twinkle, Light Conversion) and had 200 fs (FWHM) duration and 527 nm central wavelength. The input beam profile was Gaussian with a 6 mm diameter (FWHM) and formation of a single filament was induced by loosely focusing the laser pulse with a 0.5 m focal length in water and LBO cases, and with a 5 m focal length in the air case. The  $(\theta, \lambda)$  angular spectra were detected with a home-made (for the air case) or commercial imaging spectrometer (MS260i, Lot-Oriel) [13]; we underline that all measurements are single shot in order to avoid the effect of any possible input energy fluctuations that may wash out important details if averaged over many shots. Furthermore the high energies involved in the air case required that the spectra be measured by taking a reflection from a fused-silica glass plate whereas the water and LBO filaments were sent directly to the spectrometer.

In Fig. 1 we show the  $(\theta, \lambda)$  spectra for 3 cm propagation in water and with increasing input pulse energies from 1  $\mu\text{J}$  to 4  $\mu\text{J}$  (from (a) to (d)), Fig. 1(c) corresponding to an energy just above the experimentally observed threshold for filament formation. The input powers are given as a function of the self-focusing threshold power, which reads  $P_{\text{cr}} = 3.77\lambda_0^2/8\pi n_0 n_2$ , where  $n_0, n_2$  denote, respectively, the linear and nonlinear refractive indices and  $\lambda_0$  is the incident laser wavelength. For water we have  $P_{\text{cr}} \sim 1.15$  MW at 527 nm [23] so that the input power is in the range  $P \sim 4\text{--}20P_{\text{cr}}$ . Fig. 1(a) shows the Gaussian-like output spectrum in the linear regime ( $E_{\text{in}} = 1.5$   $\mu\text{J}$ ) that evolves into a butterfly-like shape at  $E_{\text{in}} = 1.8$   $\mu\text{J}$ , indicating a marked spatio-temporal focusing. For higher energies we observe a well-defined X-shaped profile (Fig. 1(c) for  $E_{\text{in}} = 2$   $\mu\text{J}$ ), characteristic of CE. As  $E_{\text{in}}$  increases further the spectrum becomes more complicated showing multiple X tails (Fig. 1(d)) and finally, for  $E_{\text{in}} > 5$   $\mu\text{J}$ , breaks up into a complicated pattern that changes from to shot-to-shot acquisitions and is interpreted as due to local breakdown inside the water medium.

We then proceeded to fit the CE tails at large  $\Omega$  allowing linear fits that do not necessarily pass through  $\theta = 0, \Omega = 0$ . This angle-shift was already noticed and linked to the effect of the nonlinear phase shift [24] but it does not affect the dispersion slope. In Fig. 1(e) we show the  $(\theta, \Omega)$  graph with the points of maximum CE gain (full circles) taken from Fig. 1(c) and the corresponding linear fit (solid line). The slope of this fit,  $60.5 \pm 1.6$  fs  $\mu\text{rad}$  is close to the value 59.4 fs  $\mu\text{rad}$  predicted by Eq. (1) using the known value for the material dispersion at 527 nm:  $k_0'' = 0.056$  fs<sup>2</sup>/ $\mu\text{m}$  [25].

We briefly note that a similar analysis has been performed on data presented elsewhere [13] regarding a lithium-triborate (LBO) crystal. The crystal, operated in the absence of quadratic nonlinear response yields a value for the slope of  $62.7 \pm 2.5$  fs  $\mu\text{rad}$  against an expected value of 64.8 fs  $\mu\text{rad}$  (corresponding to a dispersion value of  $k_0'' = 0.079$  fs<sup>2</sup>/ $\mu\text{m}$ ).

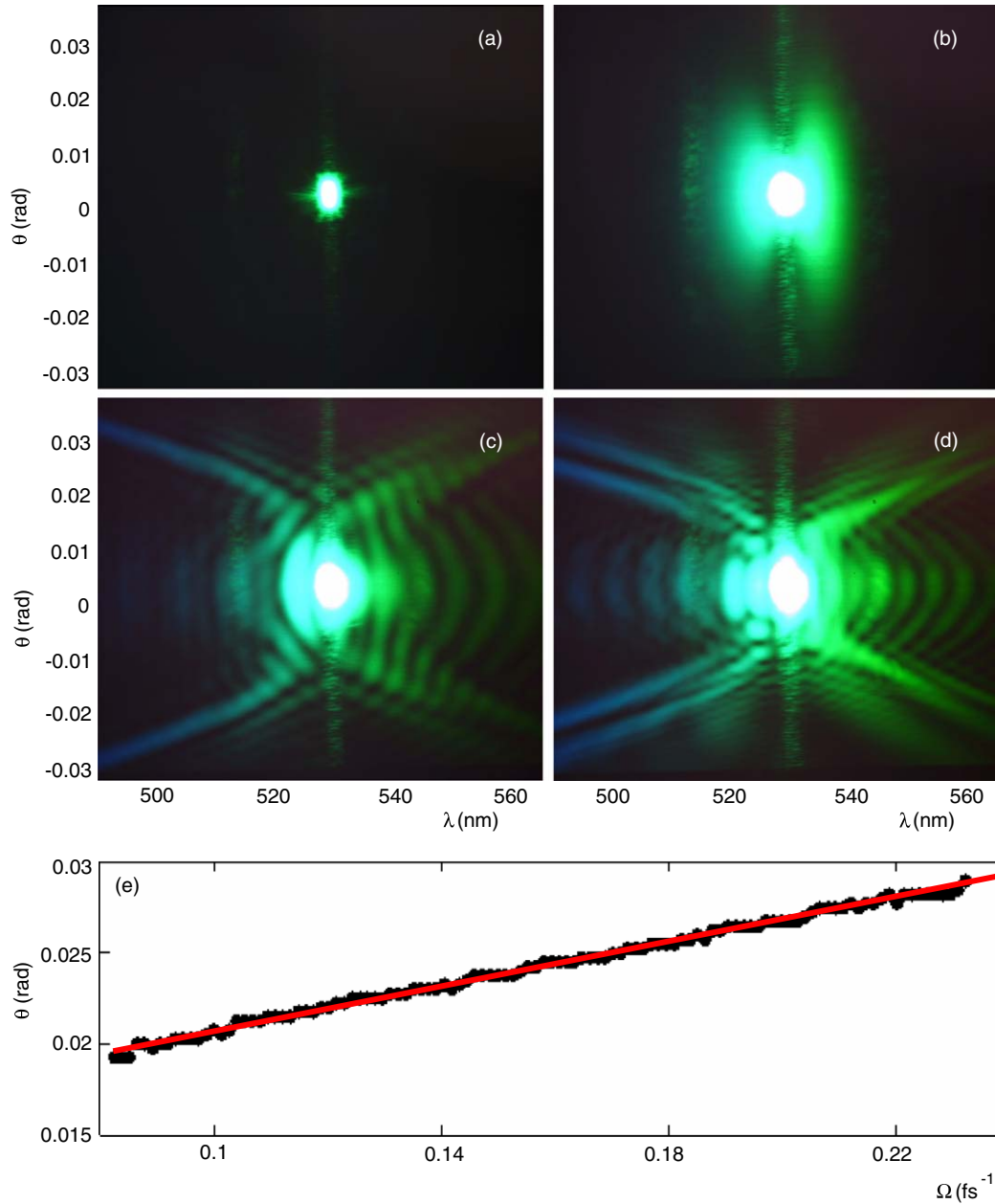


Fig. 1. Measured  $(\theta, \lambda)$  spectra (in real colors) for a filament with an input pulse of 200 fs duration, 527 nm central wavelength, in 3 cm of water at various input energies: (a)  $E_{\text{in}} = 1.5 \mu\text{J}$ , (b)  $E_{\text{in}} = 1.8 \mu\text{J}$ , (c)  $E_{\text{in}} = 2 \mu\text{J}$  and (d)  $E_{\text{in}} = 4 \mu\text{J}$ . (e) shows the points of maximum CE gain taken from (c). The solid line corresponds to the best fit. (For interpretation of the references in colour in this figure legend, the reader is referred to the web version of this article.)

The results in water were obtained with input energies just slightly higher than those necessary for experimental observation of filament formation. We have also investigated the effects of increasing input energy on CE structure. Fig. 2 shows the measured CE slope for increasing input energies. The solid circles correspond to the blue-shifted CE tails and the solid squares to the red-shifted tails. We were able to obtain a well-defined value for the red-shifted tail slope only for energies below  $E_{\text{in}} = 3 \mu\text{J}$ : above this energy the red-shifted tails broaden out so much that the fitting procedure becomes rather arbitrary (so these values are not plotted). We note that the slopes are always slightly

smaller for the red tails than for the blue ones. This fact finds explanation from third-order dispersion. In fact, following the derivation of Eq. (1) [10] but now including a third-order dispersion ( $k_0''' = \partial^3 k / \partial \omega^3|_{\omega_0}$ ) term we obtain

$$\theta = \sqrt{\frac{1}{k_0} \left( k_0'' + \frac{1}{3} k_0''' \Omega \right)} \Omega \quad (3)$$

which yields flattened red tails ( $\Omega < 0$ ) in comparison with the blue ones ( $\Omega > 0$ ) if  $k_0''' > 0$ , as in water at 527 nm. Indeed, proceeding to fit directly Eq. (3) (taking  $k_0''$  and  $k_0'''$  as free parameters) to the experimental data for  $E_{\text{in}} = 2 \mu\text{J}$

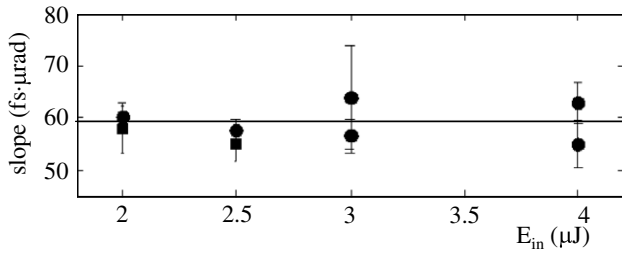


Fig. 2. Plot of retrieved CE slopes versus input pulse energy for filaments in 3 cm of water. Circles (squares) are for the blue (red) shifted tails. The solid line indicates the expected slope corresponding to the material dispersion value,  $k_0'' = 0.056 \text{ fs}^2/\mu\text{m}$ .

we obtain  $k_0'' = 0.056 \text{ fs}^2/\mu\text{m}$  and  $k_0''' = 0.03 \text{ fs}^3/\mu\text{m}$  in good agreement with  $k_0'' = 0.058 \text{ fs}^2/\mu\text{m}$  and  $k_0''' = 0.028 \text{ fs}^3/\mu\text{m}$  measured by white light interferometry [25], and confirming again that the linear dispersion of the medium determines the structure of CE.

We note that for  $E_{in} \geq 3 \mu\text{J}$  the blue-shifted tails split with slightly different values of the slope (both of which are indicated in Fig. 2 with solid circles), maintaining an overall agreement with the expected value as seen in Fig. 2. However, one might notice a general trend featuring a smooth decreasing in the slope fitting parameter on increasing the pump energy, especially if the attention is focused on the inner tails only. Among the possible physical effects that could modify the tail slope at high pumping we quote the self-generated plasma, which has been predicted to give rise to a reduction in the effective material

dispersion [26] and hence in the tail AD slope. Indeed, by assuming a plasma electron density  $\rho_e = 10^{19} \text{ cm}^{-3}$ , which is compatible with what one should expect in our operating regime [27], and by taking for granted the model proposed in the reference above, we obtained a decrease in  $k_0''$  of  $0.01 \text{ fs}^2/\mu\text{m}$ , and therefore a decrease in good agreement with our experimental results for the case of  $E_{in} = 4 \mu\text{J}$ . The argument, however, does not explain the appearance of the outer tails in the angular spectrum, for which a different justification has to be found.

We also extend the above results to filamentation in air. In Fig. 3(a) we show the  $(\theta, \lambda)$  spectrum of an air filament generated with an input pulse energy  $E_{in} = 3 \text{ mJ}$  ( $P \sim 10P_{cr}$ ), with a filament length of  $\sim 10 \text{ m}$ . In Fig. 3(b) we show the  $(\theta, \Omega)$  graph with the points of maximum CE gain (full circles) and the corresponding linear fit (solid line). The slope of this fit,  $1.5 \pm 0.2 \text{ fs } \mu\text{rad}$  is close to the value  $1.689 \text{ fs } \mu\text{rad}$  predicted by Eq. (1) using the known value for the material dispersion at  $527 \text{ nm}$ :  $k_0'' = 0.34 \text{ fs}^2/\text{cm}$  [28]. This confirms that also for the case of filamentation in air the spectrum bears compelling evidence of the spontaneous generation of X-waves. This result is not obvious due to the fact that filamentation in air is usually described in terms of a balance between Kerr induced self-focusing and plasma-induced defocusing, the latter effect being much stronger than in condensed media. Further measurements and numerical simulations will be carried out in order to ascertain the full role of self-generated plasma in our operating conditions, in particular to establish if plasma may still be considered as a perturba-

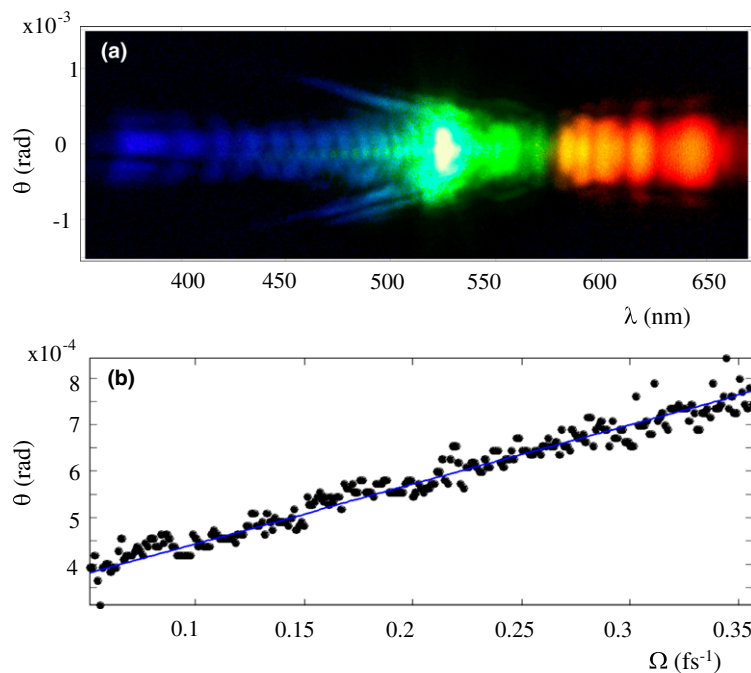


Fig. 3. (a) Measured  $(\theta, \lambda)$  spectra (in real colors) for a filament in air with an input pulse of 200 fs duration, 527 nm central wavelength and  $E_{in} = 3 \text{ mJ}$ . (b) Points of maximum CE gain taken from (a). The solid line corresponds to the best linear fit. (For interpretation of the references in colour in this figure legend, the reader is referred to the web version of this article.)

tive effect (as in condensed media) or if the plasma is even possibly contributing toward X-wave formation.

We also note that the CE associated to laser pulse filamentation in air is usually interpreted on the basis of other mechanisms, e.g. in particular Cerenkov emission [7,8]. However it is possible to show that the phase-matching condition for Cerenkov emission is equivalent to the linear X-mode relation Eq. (2). A polarization wave oscillating at frequency  $\omega'$  and excited by an input pump beam at frequency  $\omega_p$ , may travel faster than the group velocity of a light pulse at  $\omega = \omega'$ . In a manner very similar to that observed with particles traveling superluminally in a medium, the light-wave emitted by the polarization-wave will be emitted at an angle. This angle is easily determined by imposing a longitudinal (i.e., along the propagation direction  $z$ ) phase-matching condition, which is usually written in the form  $n(\omega)\cos\theta(\omega) = n_0$  [7]. Multiplying both members of this relation by  $\omega/c$ , and on account that  $\omega = \omega_0 + \Omega$ , this relation can be rewritten as  $k(\omega)\cos\theta(\omega) = k_0 + n_0\Omega/c$ . Introducing the series expansion  $k(\omega) = k_0 + k_0'\Omega + \frac{1}{2}k_0''\Omega^2 + \dots$  and  $\cos\theta = 1 - \frac{1}{2}\theta^2 + \dots$ , and retaining up to second-order terms (for paraxial angles and small detunings), we obtain

$$\theta = \sqrt{\frac{2}{k_0} \left( \alpha\Omega + \frac{1}{2}k_0''\Omega^2 \right)} \quad (4)$$

(with  $\alpha = k_0' - n_0/c$ ), which represents in fact the dispersion relation of a linear X-wave (Eq. (2)) with  $\beta = 0$ , i.e., an X-wave whose dispersion curve passes through the origin  $(\theta, \Omega) = (0, 0)$ . Indeed, although the spectral region near the origin is rather over-saturated we can still observe in both Figs. 1 and 3 that indeed the CE tails appear to pass through the origin. Therefore the interpretation of CE in terms of Cerenkov emission or in terms of spontaneous formation of X-waves are consistent with each other. The reason for this may be understood by realizing that the Cerenkov condition is a longitudinal phase-matching condition. Yet it is precisely a phase-matched Kerr interaction that will lead to the spontaneous formation of X-waves. In other words, both interpretations advocate a Kerr-mediated nonlinear process with a precise momentum conservation condition. Moreover, interpretation in terms of X-waves allows not only a description of the CE characteristics but of the whole filamentation dynamics and gives an insight also into the near-field evolution [9]. As a final comment we note that a further interpretation has been given to the CE formation dynamics in which the wavelength-dependent angular emission is described as due to strong spatiotemporal SPM [29]. We believe that it should be possible to reconcile also this description with the one given here although we reserve this task for future work.

In conclusion we have presented experimental measurements of conical emission  $(\theta, \lambda)$  spectra that clearly show how the AD slope of the CE is determined by the material dispersion. At higher input energies it is necessary to account also for higher order nonlinear effects that may

lead to a variation of the material dispersion, as observed in our spectra. This finding is in agreement with and supports the recent interpretation of filamentation dynamics in terms of spontaneous X-wave formation. These results are also extended to the case of filamentation in air. Future work will be directed at interpreting these spectra using the paradigm of X-waves that may contribute to a deeper understanding of the behavior in the central (non-asymptotic) region of the angular spectrum.

## Acknowledgements

The authors wish to acknowledge VINO (Virtual Institute of Nonlinear Optics) for fruitful discussions and financial support from FIRB01, COFIN04 projects from the Italian Ministry of University and Research (MIUR) and from Accion integrada Hispano-Italiana H12004-0078.

## References

- [1] K. Wilson, V. Yakovlev, *J. Opt. Soc. B* 14 (2) (1997) 444.
- [2] R. Alfano, *The Supercontinuum Laser Source*, Springer-Verlag, New York, 1989.
- [3] P. Rairoux, H. Schillinger, S. Niedermeier, M. Rodriguez, F. Ronneberger, R. Sauerbrey, B. Stein, D. Waite, C. Wedekind, H. Wille, L. Wöste, C. Ziener, *Appl. Phys. B* 71 (2000) 573.
- [4] P. Nozieres, D. Pines *The Theory of Quantum Liquids*, vol. II, Addison-Wesley, Redwood City, 1990.
- [5] A. Couairon, *Phys. Rev. A* 68 (2003) 015801.
- [6] Q. Xing, K. Yoo, R. Alfano, *Appl. Opt.* 32 (12) (1993) 2087.
- [7] E.T.J. Nibbering, P.F. Curley, G. Grillon, B.S. Prade, M.A. Franco, F. Salin, A. Mysyrowicz, *Opt. Lett.* 21 (1996) 62.
- [8] I. Golub, *Opt. Lett.* 156 (1990) 305.
- [9] M. Kolesik, E. Wright, J. Moloney, *Phys. Rev. Lett.* 92 (25) (2004) 253901.
- [10] G. Luther, A. Newell, J. Moloney, E. Wright, *Opt. Lett.* 19 (11) (1994) 789.
- [11] L. Liou, X. Cao, C. McKinstrie, G. Agrawal, *Phys. Rev. A* 46 (7) (1992) 4202.
- [12] J. Trull, O. Jedrkiewicz, P. Di Trapani, A. Matijosius, A. Varanavičius, G. Valiulis, R. Danielius, E. Kucinskas, A. Piskarskas, *Phys. Rev. E* 69 (2004) 026607.
- [13] D. Faccio, P. Di Trapani, S. Minardi, A. Bramati, F. Bragheri, C. Liberale, V. Degiorgio, A. Dubietis, A. Matijosius, *J. Opt. Soc. Am. B* 22 (4) (2005) 862.
- [14] P. Gabolde, R. Trebino, *Opt. Exp.* 12 (19) (2004) 4423.
- [15] W. Smith, P. Liu, N. Bloembergen, *Phys. Rev. A* 15 (6) (1977) 2396.
- [16] A. Dubietis, E. Gaizauskas, G. Tamosauskas, P. Di Trapani, *Phys. Rev. Lett.* 92 (2004) 253903.
- [17] M.A. Porras, A. Parola, D. Faccio, A. Dubietis, P. Di Trapani, *Phys. Rev. Lett.* 93 (2004) 153902.
- [18] C. Conti, S. Trillo, P. Di Trapani, G. Valiulis, A. Piskarskas, O. Jedrkiewicz, J. Trull, *Phys. Rev. Lett.* 90 (2003) 170406.
- [19] D. Faccio, A. Matijosius, A. Dubietis, R. Piskarskas, A. Varanavičius, E. Gaizauskas, A. Piskarskas, A. Couairon, P. Di Trapani, *Phys. Rev. E* 72 (2005) 037601.
- [20] A. Couairon, E. Gaizauskas, D. Faccio, A. Dubietis, P. Di Trapani, *Phys. Rev. E* 73 (2006) 016608.
- [21] M. Kolesik, E.M. Wright, J.V. Moloney, *Opt. Exp.* 13 (26) (2005) 10729.
- [22] M.A. Porras, P. Di Trapani, *Phys. Rev. E* 69 (2004) 066606.

- [23] D.N. Nikogosyan, *Properties of Optical and Laser-Related Materials*, Wiley, New York, 1997.
- [24] R. Alfano, S. Shapiro, *Phys. Rev. Lett.* 24 (11) (1970) 584.
- [25] A. Van Engen, S. Diddams, T. Clement, *Appl. Opt.* 37 (1998) 5679.
- [26] I. Koprnikov, *Appl. Phys. B* 79 (2004) 359.
- [27] This was verified by performing simulations based on the NLSE including terms for plasma generation (as described for example in [5]).
- [28] E.R. Peck, K. Reeder, *J. Opt. Soc. Am.* 62 (1972) 958.
- [29] O.G. Kosareva, V.P. Kandidov, A. Brodeur, C.Y. Chien, S.L. Chin, *Opt. Lett.* 22 (17) (1997) 1332.